Instrument Science Report WFC3 2014-01

Flux Calibration Monitoring: WFC3/IR G102 and G141 Grisms

Janice C. Lee, Norbert Pirzkal, Bryan Hilbert
January 24, 2014

ABSTRACT

As part of the regular WFC3 flux calibration monitoring program, we analyze WFC3/IR G102 and G141 grism observations of the standard star GD153 taken in 2013June (Cycle 20 Program 13092). The IR grism flux calibrations for the +1 order spectra are shown to have excellent temporal stability over WFC3's 4 years of operation, with average variations constrained to be less than 1%. Tests of the current corrections for throughput variations over the field-of-view and aperture losses are also performed, and no significant changes are found. These results confirm that the G102 and G141 sensitivity functions and flat-field cubes currently in use for +1 order spectra are still valid.

1. Introduction

Flux calibration of the two WFC3/IR grisms, G102 and G141, which cover wavelengths from 800-1150 nm and 1100-1700 nm respectively, was initially performed during ground testing (Kuntschner et al. 2008a,b; Kuntschner et al. 2009), and then revised based upon SMOV and Cycle 17 observations (Kuntschner et al. 2011). Since detectors and optical systems suffer gradual degradation in sensitivity, regular monitoring of the flux calibration must be performed. In this report, we present an analysis of Cycle 20 WFC3/IR grism observations of the HST primary flux standard GD153 (Program ID 13092) as part of our regular monitoring program to check for possible changes in the calibration over time. This analysis uses the sensitivity functions available at http://www.stsci.edu/hst/wfc3/analysis/grism_obs/wfc3-grism-resources.html, which were also based on observations of GD153. This report focuses on

calibration stability of the +1 order spectrum; other orders will be considered in subsequent work from the WFC3 team.

2. Observations

On 2013 June 1, two orbits allocated to the HST Cycle 20 WFC3 calibration program 13092 were used to obtain G102 and G141 grism spectra of the white dwarf spectrophotometric standard star GD153 at three positions on the IR detector (Figure 1). Grism observations at each position are immediately preceded by direct images in broadband filters which overlap the wavelength range covered by the grisms (F098M and F105W for G102, and F140W and F160W for G141). Grism observations near the center of the FOV consist of a set of four sub-arcsec dithered exposures, while two dithered grism exposures are taken at the other positions. Essential information about the data obtained for this analysis are listed in Table 1. We note that GD153 was chosen instead of GD71 (which has been observed in previous WFC3 grism calibration programs) for this analysis because it is better isolated, and more immune to contamination by spectral overlap from fainter neighboring objects (Lee et al. 2012).

3. Data Reduction

Observations of GD153 from HST Program 13092 were retrieved from the Mikulski Archive for Space Telescopes (MAST). The HST "calwf3" pipeline-processed "flt" data (Table 1) were fed through the aXe grism data reduction package. We use aXe version 2.4 for this analysis. This version of aXe (available beginning with the 2013-06-06 release of IRAFX) updates the "iolprep" task for compatibility with the AstroDrizzle package, which is intended to replace MultiDrizzle for image stacking. The iolprep task computes the positions of undispersed sources, specified in a catalog constructed from a deep drizzled image of the field, in the coordinate system of the direct images taken prior to each grism observation. These positions provide anchors for the wavelength zeropoint of the spectra in the grism observations. The positions are computed using the astrometric information stored in the drizzled image file, the storage format of which has changed in AstroDrizzle data products, necessitating a corresponding update to the iolprep task. To test and verify the iolprep-associated code changes[1], we also process the data using MutliDrizzle and aXe version 2.3, available through STSDAS 3.14. We confirm that the two versions of the software yield direct image positions that are identical within 0.1 pixel.

[1] More information on aXe software version updates is available at: http://axe-info.stsci.edu/extract_calibrate

Table 2 lists the aXe configuration files (providing trace and wavelength solutions), and the flat-field and master sky files that were used in the reduction. The current WFC3/IR grism +1st order calibration and reference files are primarily based on grism data taken during Cycle 17 WFC3 Servicing Mission Orbital Verification (SMOV) and have not changed since then (Kuntschner et al. 2011). The current flat-field calibration accounts for large-scale variations in the throughput, using a relative correction to the v1 flat field based upon Cycle 17 11936 observations of GD71 at nine positions over the FOV (Kuntschner et al. 2008; 2011).

aXe performs the requisite background subtraction, automated spectral extraction, calibration, combination of multiple exposures for +1st order spectra ("drizzling"), and provides both 1-dimensional spectra and 2-dimensional rectified spectral images. The spectra are extracted in a fixed direction perpendicular to the trace, and with twelve total widths spanning from 0″.128 (1 pixel) to 25″.6 (200 pixels) as listed in Table 3. These extraction widths correspond to those used in Kuntschner et al. (2011; Table 6) to compute point source aperture corrections, which are also checked in this analysis.

4. Analysis

4.1 Temporal Stability

We examine the stability of the flux calibration of the G102 and G141 grisms, using the most recent model of GD153, which is available through the STScI Calibration Database System "Calspec[2]." Figure 3 shows the results of the extraction. For comparison, we also show spectra based on calibration observations taken during the previous two HST cycles (18 and 19) as well as during Servicing Mission Orbital Verification (SMOV) in Cycle 17, which have been extracted with the same methods described above. Altogether the observations span the period from 2009 August to 2013 June. In Cycle 18 and 19, GD71 was observed instead of GD153, and the appropriate model spectra were obtained from Calspec for the analysis of those data.

In Figure 3, the top panel plots the spectra in units of e-/s. The middle panel plots the spectra in flux units, which are calculated by applying the current v2 sensitivity functions based on SMOV observations of GD153 (Table 2). Finally, the bottom panel shows the ratio (smoothed, in a sliding 7 pixel window) of the observed, fluxed spectra, to the model spectra. For all spectra shown in Figure 3, the standard star is observed near the center of the detector with four sub-arcsec dithered exposures, and the total extraction width is ~4″.

The validity of the v2 sensitivity functions is confirmed by the bottom panel of Figure 3. The GD153 spectra from the current Cycle 20 data are shown in black. The ratios of the observed-to-

[2] http://www.stsci.edu/hst/observatory/cdbs/calspec.html

model fluxes are close to unity and have small dispersions (less than ~1%). Aperture corrections have not been applied to the plotted spectra, so the observed spectra yield fluxes that are low in comparison with those expected from the model. When the average and standard deviation of the smoothed ratio is computed between wavelengths where the total throughput is above 10% (804-1153 nm and 1081-1691; Kuntschner et al. 2011), their values are 0.979 +/- 0.005 and 0.977 +/- 0.005 for the G102 and G141 grisms respectively. The average ratios can be compared with the Cycle 19 values of 0.985 +/- 0.005 and 0.984 +/- 0.004, and the Cycle 18 values of 0.988 +/- 0.005 and 0.988 +/- 0.004 (again each for the G102 and G141 grisms respectively). Thus, it is clear that WFC3/IR grism flux calibrations for the +1 order have been temporally stable to better than 1% over the four years that the instrument has been in operation.

4.2 Stability over FOV

Next, we examine the GD153 +1 order spectra obtained at the two off-center field positions shown in Figure 1. The reduction and extraction was performed as above, except that only two exposures are taken at each position. The results are presented in Figure 4, where the bottom panel compares the +1 order spectra from the off-center positions with the ones taken near the center of the FOV, as shown in the previous figure.

The average value of the observed-to-model ratios vary between these three positions by ~0.05%, whereas the variations described by the Kuntschner et al. (2011) throughput correction are on the order of 2% at these locations. From the top to the bottom on the detector, the average ratios for each pointing are 0.982 +/- 0.008, 0.979 +/- 0.005, 0.978 +/- 0.008 for G102, and 0.971 +/- 0.007, 0.977 +/- 0.005, 0.973 +/- 0.006 for G141. These results confirm that the current flat field correction is still valid, at least over the regions probed by our observations.

4.3 Aperture Corrections

Finally, we check the point source aperture corrections presented in Kuntschner et al. (2011) using the axedrizzled Cycle 20 observations of GD153 taken at the center of the detector. The correction is computed by taking the ratio of the flux in a given aperture to the flux measured in the largest total extraction aperture of ~200 pixels. We use twelve apertures with total widths spanning from 0″.128 (1 pixel) to 25″.6 (200 pixels), and compute the corrections at six different wavelengths, which correspond to those used in Kuntschner et al. 2011 (Table 3). It should be noted however that in both this and the Kuntschner et al. 2011 analysis, the largest aperture is contaminated by flux from another source (see lower half of the aperture in Figure 2). The flux from the contaminating source is ~0.3% the total flux of GD153.

In Figures 5 and 6, the ratio of the Kuntschner et al. (2011) aperture correction to the ones obtained here are plotted for each of the aperture widths (red points), with each panel showing

the results at a particular wavelength. The consistency between the corrections is generally within 1%, with differences of up to 2% observed for the smallest apertures (due to uncertainties in the trace and centering of the extraction aperture) and at the red end of the wavelength range of each of the grisms.

5. Conclusions

In this report, WFC3/IR G102 and G141 grism observations of GD153 in Cy 20 are analyzed and compared with standard star observations from previous cycles to monitor for changes in the current flux calibration for +1 order spectra. No significant changes are found, and variations for spectra taken near the center of the FOV continue to be less than 1%. These results again confirm the validity of the v2 WFC3/IR G102 and G141 sensitivity functions and flat-field cubes for +1 order spectra which are currently in use and are provided on the WFC3 instrument webpages. Future reports will re-evaluate the spectral trace and its variation over the FOV, and the calibration of the non +1 orders.

Acknowledgements

We thank Gabe Brammer for reviewing a draft of this report.

References

Dressel, L. & the WFC3 Team, 2013, WFC3 Instrument Handbook (IHB)

Kuntschner, H., Kummel, M., Walsh, J.R. & Bushouse, H. 2011, WFC3 Instrument Science Report, WFC3-2011-05: Revised Flux Calibration of the WFC3 G102 and G141 Grisms

Kuntschner, H., Bushouse, H., Kummel, M., & Walsh, J.R. 2009a, WFC3 Instrument Science Report, WFC3-2009-18: WFC3 SMOV proposal 11552: Calibration of the G102 grism

Kuntschner, H., Bushouse, H., Kummel, M., & Walsh, J.R. 2009b, WFC3 Instrument Science Report, WFC3-2009-17: WFC3 SMOV proposal 11552: Calibration of the G141 grism

Kuntschner, H., Bushouse, H., Walsh, J.R. & Kummel, M. 2008a, WFC3 Instrument Science Report, WFC3-2008-16: The TV3 Ground Calibrations of the WFC3 NIR Grisms

Kuntschner, H., Bushouse, H., Walsh, J.R. & Kummel, M. 2008b, WFC3 Instrument Science Report, WFC3-2008-16: The TV2 Ground Calibrations of the WFC3 NIR Grisms

Lee, J.C., Prizkal, N., Hilbert, B. 2012, WFC3 Instrument Science Report, WFC3-2012-06: Flux Calibration Monitoring: WFC3/IR G102 and G141 Grisms

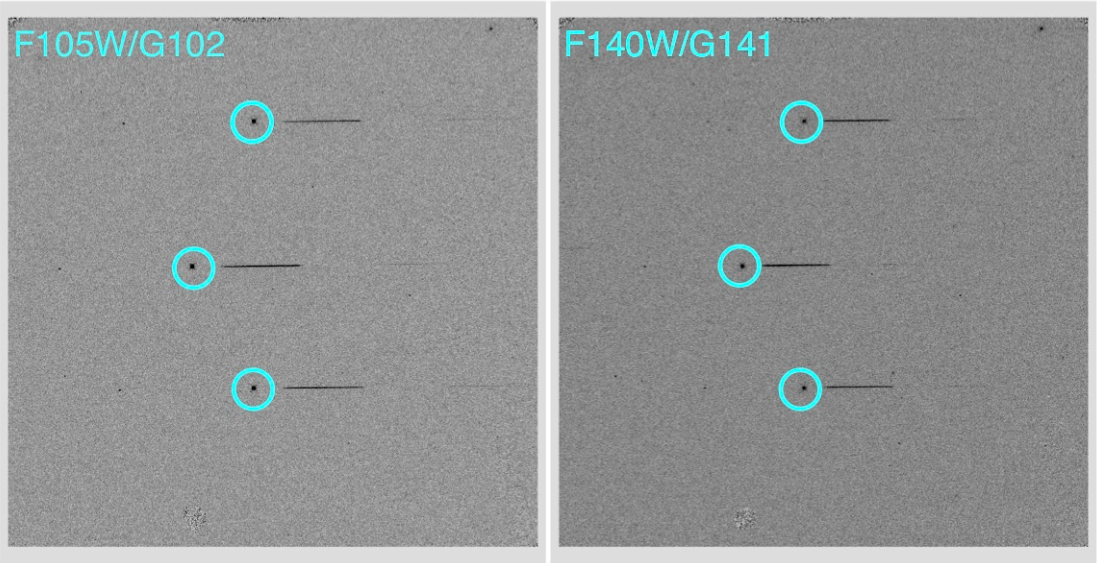

Figure 1: In calibration program 13092, grism spectra and direct images of GD153 are taken at three locations on the IR detector to monitor the temporal stability and test for variability of the flux calibration over the field-of-view. The grism and preceding broadband images at the three pointings have been simply summed to produce these composite images, which also serve to illustrate the relative positioning of the direct (circled) and +1st order spectra. 0th and +2 order spectra are faint but visible on the left and right sides of the detector, respectively. Four dithered grism exposures are taken at the central pointing, while two are taken at each of the two other pointings.

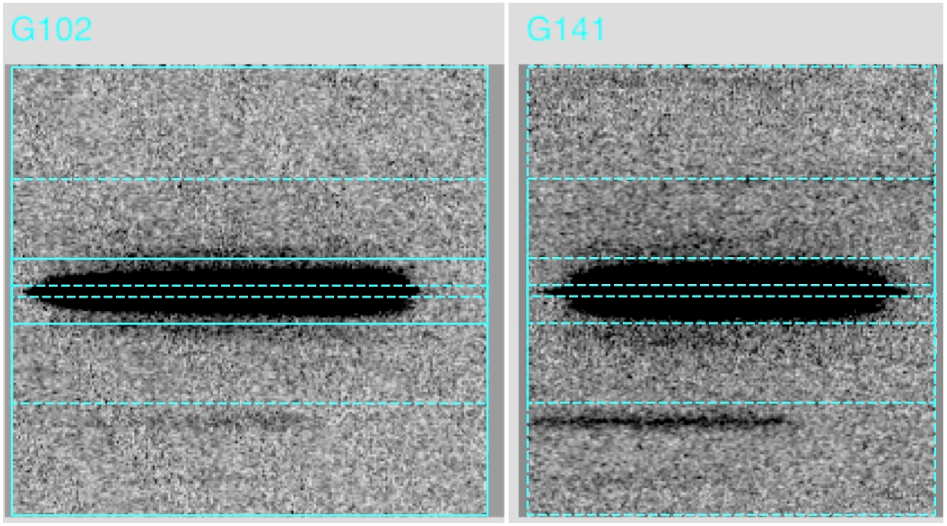

Figure 2: aXedrizzled 1st order GD153 spectra generated from four sub-pixel dithered grism images taken near the center of the field-of-view obtained in calibration program 13092. The images are from aXedrizzled "STP" files where the total width of the extraction box is 200 pixels (~26″; largest cyan box). Eleven additional smaller sub-apertures are also extracted to enable a curve-of-growth analysis to test the aperture correction given in Kuntschner et al. (2011); three of these sub-apertures are also shown (5, 30, 100 pixels; corresponding to 0″.64, 3″.7, 13′.). GD153 is a well-isolated star, and contamination from the spectra of other sources is insignificant within 50 pixels of the trace.

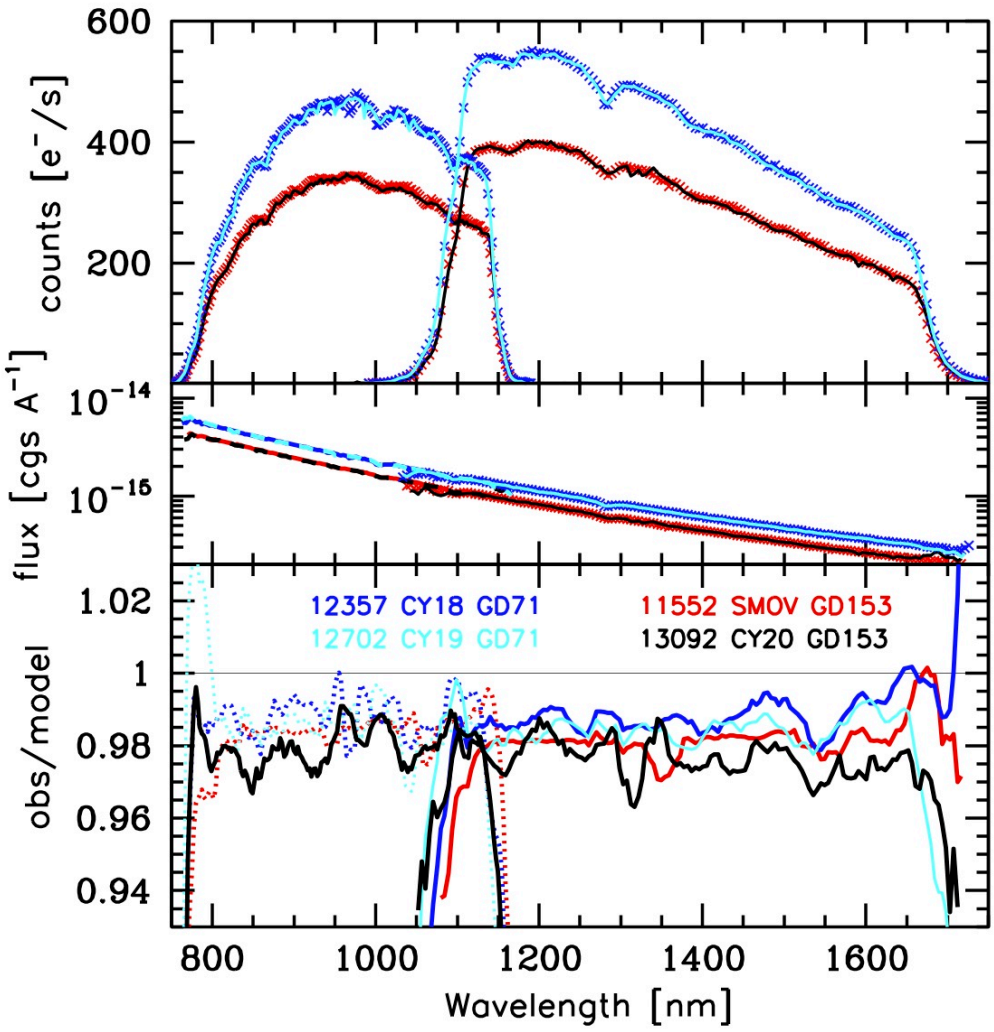

Figure 3: Monitoring of the current WFC3/IR "v2" flux calibration of +1 order spectra for the G102 grism (left set of curves) and the G141 grism (right set of curves). Spectra from the initial Servicing Mission Orbital Verification (SMOV) calibration program, and those from all three cycles following SMOV are presented. The top panel shows the aXe extracted 1-dimensional spectra of the targeted standard stars (GD71 and GD153), based on four slightly dithered observations taken at the center of the FOV which have been aXedrizzled together. The middle panel plots the spectra in flux units, which are calculated by applying the current v2 sensitivity functions based on SMOV observations of GD153. The bottom panel shows the ratio of the observed flux to the model spectrum. The total width of the extraction aperture is ~4″.

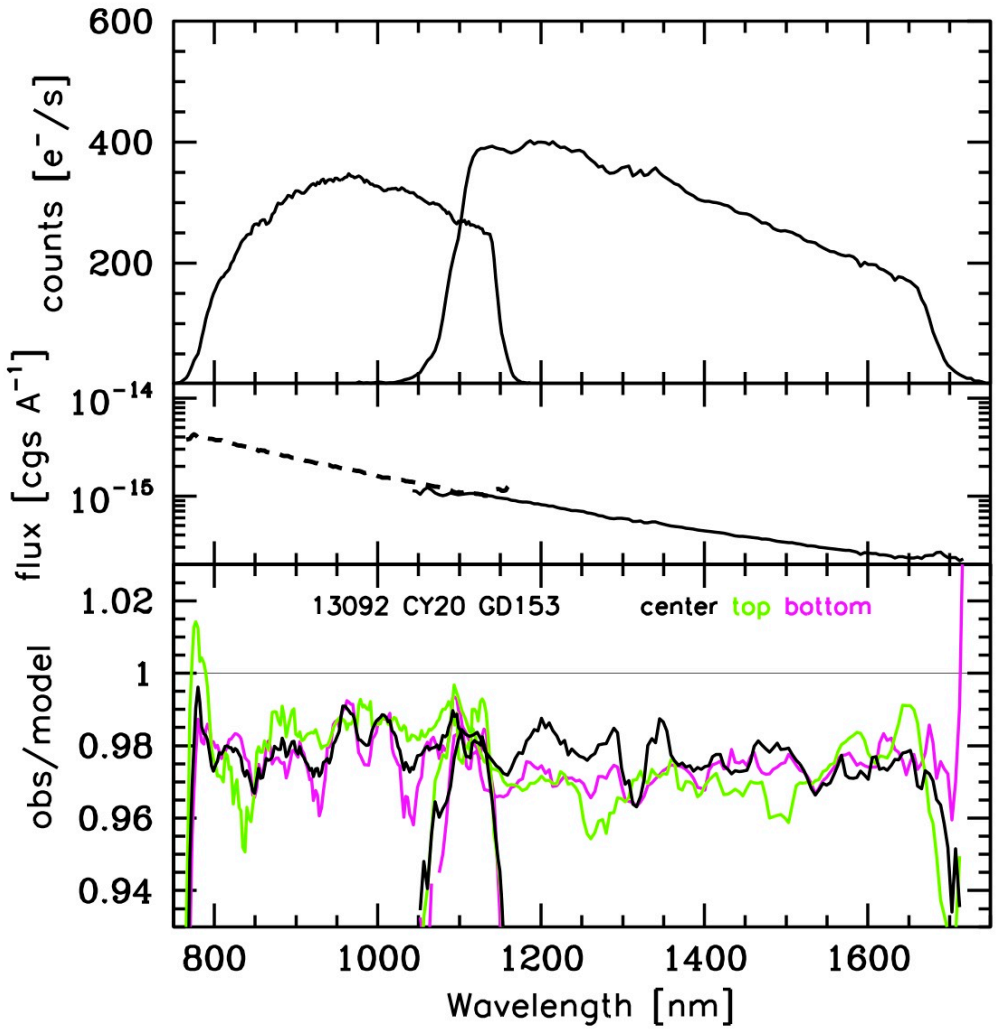

Figure 4: Same as Figure 3, but with spectra of GD153 taken at two off-center positions (see Figure 1) overplotted in the bottom panel.

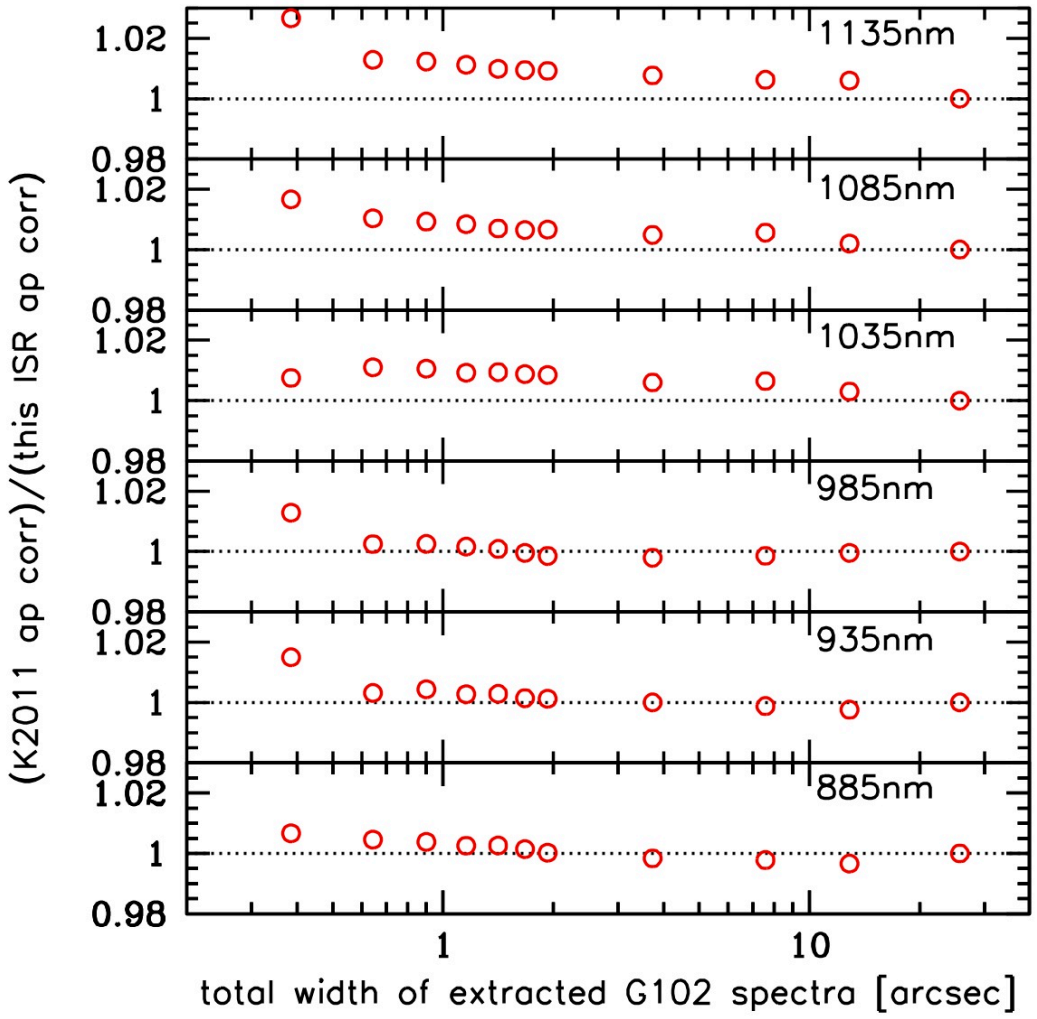

Figure 5: Comparison of aperture corrections for the G102 spectra given in Kuntchner et al. (2011) with aperture corrections computed based on the Cycle 20 13092 data. The red points show the ratios of the two aperture corrections for 11 extraction widths from 0″.38 to 25″.7 (see Table 3), and measured at 6 different wavelengths as indicated in each panel.

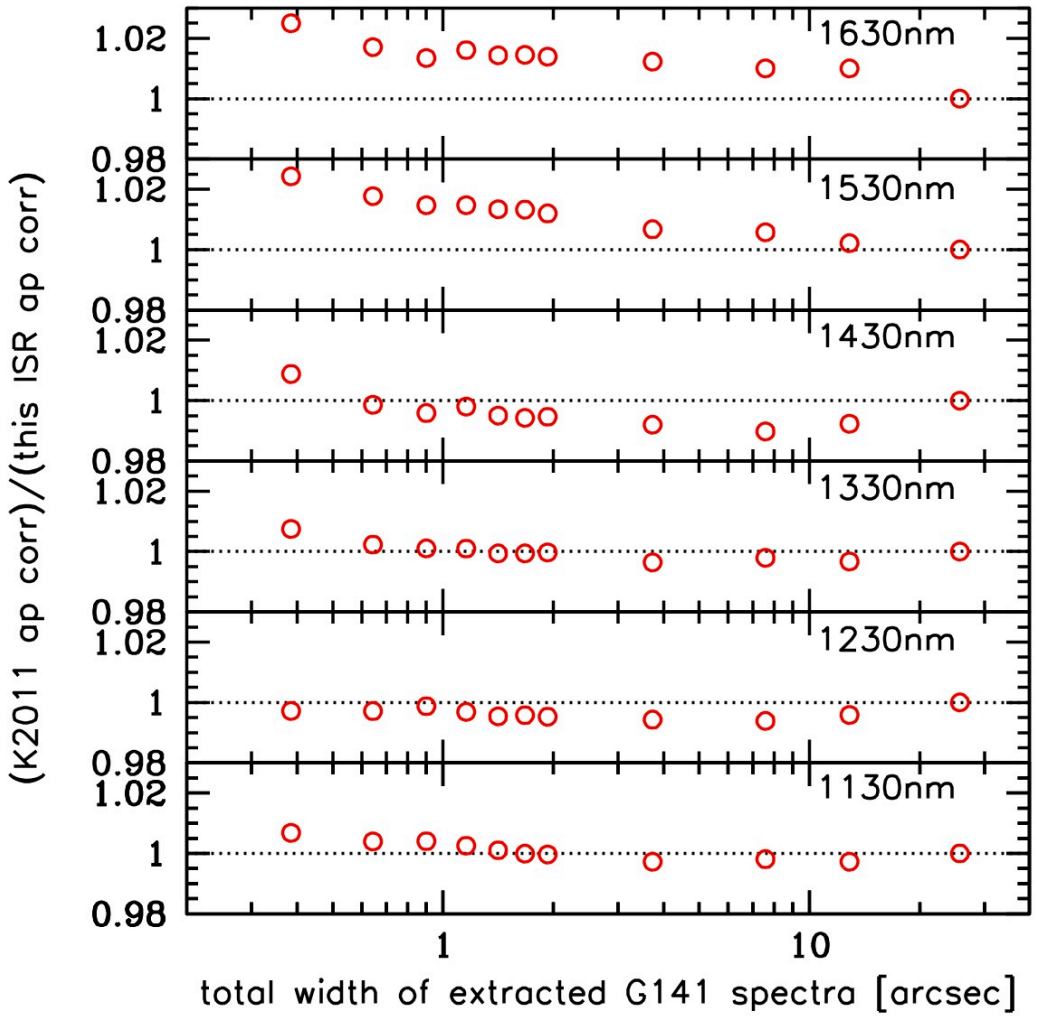

Figure 6: Same as Figure 5 but for the G141 spectra.

CY20-13092 GD153 DATE-OBS: 2013-06-1					
FILENAME	FILTER	EXPTIME (s)	TIME-OBS (UT)	POSTARG1 (arcsec)	POSTARG2 (arcsec)
ic461aghq_flt	F098M	5.86	08:15:17	-20.00	0.00
ic461agiq_flt	F105W	2.93	08:15:50	-20.00	0.00
ic461agjq_flt	G102	102.93	08:16:22	-20.00	0.00
ic461aglq_flt	G102	102.93	08:19:09	-20.00	2.00
ic461agmq_flt	G102	102.93	08:21:59	-20.00	-2.00
ic461agnq_flt	G102	102.93	08:24:47	-20.00	0.50
ic461agpq_flt	F098M	5.86	08:37:36	-4.00	-28.00
ic461agqq_flt	F105W	2.93	08:38:09	-4.00	-28.00
ic461agrq_flt	G102	102.93	08:38:41	-4.00	-28.00
ic461agsq_flt	G102	102.93	08:41:28	-4.00	-26.00
ic461agtq_flt	F098M	5.86	08:44:44	-4.00	34.00
ic461aguq_flt	F105W	2.93	08:45:17	-4.00	34.00
ic461agvq_flt	G102	102.93	08:45:49	-4.00	34.00
ic461agwq_flt	G102	102.93	08:48:36	-4.00	36.00
ic461ah4q_flt	F140W	5.86	09:36:00	-20.00	0.00
ic461ah5q_flt	F160W	5.86	09:36:44	-20.00	0.00
ic461ah6q_flt	G141	102.93	09:37:19	-20.00	0.00
ic461ah7q_flt	G141	102.93	09:40:06	-20.00	2.00
ic461ah8q_flt	G141	102.93	09:42:56	-20.00	-2.00
ic461ah9q_flt	G141	102.93	09:45:44	-20.00	0.50
ic461ahbq_flt	F140W	5.86	09:58:52	-4.00	-28.00
ic461ahcq_flt	F160W	5.86	09:59:36	-4.00	-28.00
ic461ahdq_flt	G141	102.93	10:00:11	-4.00	-28.00
ic461aheq_flt	G141	102.93	10:02:58	-4.00	-26.00
ic461ahfq_flt	F140W	5.86	10:06:14	-4.00	34.00
ic461ahgq_flt	F160W	5.86	10:06:58	-4.00	34.00
ic461ahhq_flt	G141	102.93	10:07:33	-4.00	34.00
ic461ahjq_flt	G141	102.93	10:20:41	-4.00	36.00

Table 1: Files from the Cycle 20 calibration program 13902 which are used in this analysis with basic information taken from the image headers. The "POSTARG" columns give offset values along orthogonal axes that are essentially parallel to the edges of the IR detector (see Dressel et al. 2013, IHB section 7.4.3), relative to the reference pixel for the GRISM1024 aperture (see IHB section 7.4.5).

File Name	Description
WFC3.IR.G102.V2.0.conf	configuration files
WFC3.IR.G141.V2.5.conf	
WFC3.IR.G*.flat.2.fits	flat-field cubes
WFC3.IR.G*.sky.V1.0.fits	master sky images
WFC3.IR.G*.0th.sens.1.fits	0th order sensitivity functions
WFC3.IR.G*.1st.sens.2.fits	+1st order sensitivity functions
WFC3.IR.G*.2nd.sens.2.fits	+2nd order sensitivity functions
WFC3.IR.G*.3rd.sens.2.fits	+3rd order sensitivity functions
WFC3.IR.G102.m1st.sens.2.fits	−1st order sensitivity functions
WFC3.IR.G141.m1st.sens.2.5.fits	

Table 2: A listing of WFC3 IR grism calibration files used with the aXe package to process the observations taken in Cycle 20 calibration program 13902.

extrfwhm [pix]	drzfwhm [pix]	width*a (OAF file) [pix]	total width [arcsec]
-1.53	-0.53	0.50	0.13
-2.59	-1.59	1.50	0.38
-3.65	-2.65	2.50	0.64
-4.71	-3.71	3.51	0.64
-5.77	-4.77	4.51	0.90
-6.83	-5.83	5.51	1.16
-7.89	-6.89	6.51	1.41
-8.95	-7.95	7.51	1.67
-16.37	-15.37	14.52	1.93
-32.27	-31.27	29.55	3.72
-54.0	-53.0	50.08	12.85
-107.0	-106.0	100.16	25.69

Table 3: The parameter values in the axecore and axedrizzle tasks that were specified for the extraction width from the individual exposures (extrfwhm), and the extraction width from the drizzled, combined grism images (drzfwhm). The negative sign instructs axe to use fixed extraction apertures, rather than apertures with variable widths based on the target angular diameter. These values give the number of pixels on each side of the trace to include in the extraction. The resulting extraction width on each side of the trace as reported in the axedrizzle output OAF file is also listed. Hence, the total width (in pixels) of the extracted spectra is twice the value given in the third column. The pixel scale, 0.1282 arcsec/pix, in the cross dispersion direction is used to calculate the total width of the extracted spectra, which is listed in the last column.